Observable gravitational waves from inflation with small field excursions

Shaun Hotchkiss,[a] **Anupam Mazumdar**[b] **and Seshadri Nadathur**[c]

[a]Department of Physics, University of Helsinki and Helsinki Institute of Physics, P.O. Box 64, FIN-00014 University of Helsinki, Finland

[b]Physics Department, Lancaster University, Lancaster LA1 4YB, UK
Niels Bohr Institute, Copenhagen, Blegdamsvej-17, Denmark

[c]Rudolf Peierls Centre for Theoretical Physics, University of Oxford, Oxford OX1 3NP, UK

E-mail: shaun.hotchkiss@helsinki.fi, a.mazumdar@lancaster.ac.uk, seshadri@thphys.ox.ac.uk

Abstract. The detection of primordial gravitational waves, or tensor perturbations, would be regarded as compelling evidence for inflation. The canonical measure of this is the ratio of tensor to scalar perturbations, r. For single-field slow-roll models of inflation with small field excursions, the Lyth bound dictates that if the evolution of the slow-roll parameter ϵ is monotonic, the tensor-to-scalar ratio must be below observationally detectable levels. We describe how non-monotonic evolution of ϵ can evade the Lyth bound and generate observationally large r, even with small field excursions. This has consequences for the scalar power spectrum as it necessarily predicts an enhancement in the spectrum at very small scales and significant scale-dependent running at CMB scales. This effect has not been appropriately accounted for in previous analyses. We describe a mechanism that will generically produce the required behaviour in ϵ and give an example of this mechanism arising in a well-motivated small-field model. This model can produce $r \geq 0.05$ while satisfying all current observational constraints.

Contents

1   Introduction

The positive detection of stochastic gravitational waves or tensor perturbations of the metric, especially at very large angular scales, would be considered strong evidence in favour of the inflationary paradigm [1]. The Planck satellite will be able to detect the effects of primordial gravitational waves on the CMB if the ratio of tensor to scalar perturbations, $r \equiv \mathcal{P}_{grav}/\mathcal{P}_{\zeta}$, where $\mathcal{P}_{grav}$ and $\mathcal{P}_{\zeta}$ denote the power spectra for tensor and scalar modes respectively, is $r \gtrsim 0.05 - 0.1$ [2]. It is however difficult to generate detectably large tensor perturbations in a reasonable model of inflation which is embedded within a fundamental physics framework, especially in supergravity theories, where the cut-off of the theory is always assumed to be the four-dimensional Planck scale $M_{\rm P} \simeq 2.4 \times 10^{18}$ GeV [3].

The tensor-to-scalar ratio r depends on only one of the slow-roll parameters, ϵ. In most models of inflation, ϵ increases monotonically, from a value that is necessarily small during the observational window to $\epsilon \sim 1$ at the end of inflation. Assuming such monotonic behaviour, an upper bound may be placed on the value of r, known as the Lyth bound [4]:

$$r \lesssim 0.003 \left(\frac{50}{N} \right)^2 \left(\frac{\Delta \phi}{M_{\rm P}} \right)^2 . \tag{1.1}$$

Here, $\Delta \phi$ is the change in the inflaton field value in N Hubble times (e-folds). Most scenarios require $N \sim 50$ e-folds so that, with $\Delta \phi < M_{\rm P}$, r cannot take a value large enough to ever be observed in CMB experiments. This has resulted in the widely held perspective that it is *impossible* for small-field models of inflation to generate observable gravitational waves.

A significant tensor to scalar ratio, $r \sim 0.1$, can be obtained in large-field models of inflation, such as "chaotic inflation" [5]. In this class of models, slow-roll inflation occurs when the inflaton vacuum expectation value (VEV) exceeds the Planck scale, so that $\Delta \phi \sim 5\text{-}10$ $M_{\rm P}$ is possible. However, even a gauge singlet inflaton must have couplings to the Standard Model (SM) degrees of freedom [6] which can generate corrections to any given inflaton potential. An effective field theory treatment makes no sense above the cut-off scale of quantum gravity; therefore a complete large field model of inflation must necessarily also be fully embedded in a quantum gravity framework such as string theory. While the quantum gravity framework allows the field to take super-Planckian values consistently it also introduces many additional degrees of freedom that must be kept under control. Some progress has been made in this direction [7], but a full model is still a work in progress [8].[1]

Large tensor perturbations ($r \sim 0.01\text{-}0.1$) can also be obtained with sub-Planckian field values in assisted inflation scenarios [10–12], where multiple scalar fields collectively drive inflation. Assisted

---

[1]One problem for these models is that the inflaton does not couple to the Standard model quarks and leptons directly. Also, there are many more hidden degrees of freedom which can get excited after the end of inflation. This is a characteristic of any model where a closed string modulus is used as an inflaton [9]. It is also not clear whether inflaton couplings to background fluxes and matter fields would further ruin the flatness of the potential [7].

inflation has found many examples within field theory [12], and in string motivated examples [13, 14]. However, these models require as many as 10^4-10^6 fields with the same mass to drive inflation simultaneously, making them less attractive.

These problems combined with the fact that the detection of gravitational waves is a major observational goal means it is worth examining more closely whether an observable tensor-to-scalar ratio can occur in any small-field models of inflation with a single inflaton field. It would appear that the Lyth bound negates this possibility. However, there are two ways to evade this bound. It was argued in [15] that if we drop the requirement that a single period of inflation both generates the observable perturbations and the subsequent inflationary expansion then N can be as low as ~ 8 and a single, small field inflation model *can* generate an observably large value of r. The only necessary condition for this is that a Taylor expansion of the potential around the point of inflation is dominated by a linear term. The unattractive feature of such a model is that some extra inflationary epoch is necessary to generate the observed homogeneity of the universe.

The only remaining possibility for evading the Lyth bound is to drop the assumption of the monotonic evolution of ϵ. All inflationary models with $\phi \leq M_P$ and $N \gtrsim 50$ that predict observable r *must* violate this assumption. Some examples have recently been discussed in the literature [16–20].

In this paper we explore the consequences of the non-monotonic behaviour in ϵ for the scalar power spectrum in such models. In section 2, we explain how non-monotonicity of ϵ allows the Lyth bound to be violated, what features are necessary in ϵ to also match current observations, and what new observational consequences are expected. We also argue that the required behaviour in ϵ is relatively common when a constant vacuum energy is added to a potential that supports inflation and a hybrid mechanism is included to bring inflation to an end

On CMB scales these models generically predict a non-negligible and scale-dependent running of the power spectrum. The scale-dependence of the running means it is not usually appropriate to match the power spectrum parameters to the constraints from WMAP [21] only at the pivot scale. It also provides a potentially distinct observational characteristic of small-field inflation models in the case that gravitational waves are observed. In addition, we note that these models generically provide a significant enhancement of power on very small scales, which may result in generation of primordial black holes (PBHs). These are features that are not present in other models which predict large gravitational wave signals.

Although our argument in section 2 is relevant to any small-field models that evade the Lyth bound in this manner, in section 3 we use a specific model of the scalar potential to better illustrate these features. This potential is different to the previous examples considered in the literature. We show that it can lead to a tensor-to-scalar ratio as large as $r \geq 0.05$ with $\phi \leq M_P$ while also satisfying current observational constraints. In section 3.2 we discuss how this potential may arise in a fundamental physics framework. Finally, we provide a discussion and summary in section 4.

2 Large tensor to scalar ratio and non-monotonic evolution of ϵ

The production and evolution of tensor fluctuations during inflation is equivalent to that for the fluctuations of a massless scalar field. The power spectrum is therefore given by

$$\mathcal{P}_{\text{grav}}(k) = \frac{1}{M_P^2}\left(\frac{2H^2}{\pi^2}\right)\bigg|_{k=aH}. \tag{2.1}$$

This depends only on the scale of inflation, through the Hubble parameter H. Therefore a successful detection of primordial gravitational waves from inflation immediately tells us the inflationary energy scale. In terms of the slow-roll parameters

$$\epsilon \equiv \frac{M_P^2}{2}\left(\frac{V'}{V}\right)^2, \qquad \eta \equiv M_P^2 \frac{V''}{V}, \tag{2.2}$$

the power spectrum and spectral index of scalar fluctuations produced during inflation is given, to first order in the slow-roll parameters, by

$$\mathcal{P}_\zeta(k) = \frac{1}{M_\mathrm{P}^2}\left(\frac{H^2}{8\pi^2\epsilon}\right)\bigg|_{k=aH} \quad \text{and} \quad n_s = \frac{d\ln\mathcal{P}_\zeta(k)}{d\ln k} = 1 + 2\eta - 6\epsilon\,. \tag{2.3}$$

Additionally, the running of the scalar spectral index is, to leading order in the slow-roll parameters, given by

$$\alpha \equiv \frac{dn_s}{d\ln k} = -16\epsilon\eta + 24\epsilon^2 + 2\xi^2\,, \tag{2.4}$$

where $\xi \equiv M_\mathrm{P}^4 V'V'''/V^2$. The ratio of tensor to scalar fluctuations, r, and the spectral index of the tensor fluctuations are given by the simple expressions

$$r \equiv \frac{\mathcal{P}_\mathrm{grav}}{\mathcal{P}_\zeta} = 16\epsilon\,, \quad n_t = \frac{d\ln\mathcal{P}_\mathrm{grav}(k)}{d\ln k} \simeq -2\epsilon\,. \tag{2.5}$$

These expressions depend only on ϵ. Therefore, if they could both be observed they provide a very useful consistency condition for single-field, slow-roll inflation. It is expected that Planck could detect gravity waves if $r \gtrsim 0.1$. An ideal future CMB polarisation experiment would be able to detect $r \gtrsim 10^{-2}$. However the tensor spectral index will be hard to measure because of secondary anisotropies at smaller scales.

The number of e-foldings of inflation, defined as $N = \int H\,dt$, that occur between the field value ϕ_CMB and the end of inflation can be written as

$$N = \int_{\phi_\mathrm{CMB}}^{\phi_\mathrm{e}} \frac{d\phi}{\sqrt{2\epsilon}} = \int_{\phi_\mathrm{CMB}}^{\phi_\mathrm{e}} \sqrt{\frac{8}{r}}\,d\phi\,, \tag{2.6}$$

where ϕ_e is the field value at which inflation ends and we have used the slow-roll approximation $\dot\phi/H \simeq \sqrt{2\epsilon}$. If ϵ is fixed or increasing throughout inflation this can be translated into a bound on r at horizon scales [4],

$$r_\mathrm{HOR} < 0.003\,(50/N)^2\,(\Delta\phi/M_\mathrm{P})\,. \tag{2.7}$$

This is the Lyth bound as discussed above. It is clear that if we require $N \geq 50$ and $\Delta\phi \leq M_\mathrm{P}$ then $r \leq 10^{-3}$, suggesting that no single field model of inflation with small field excursion can generate observable gravitational waves. When additional constraints provided by considerations of naturalness and the observations of the spectral index are included, this bound becomes even stronger [15].

Note that the current observational window corresponds to only ~ 8 of the total number of e-folds we require. Using $N = 8$ in eq. (2.7) gives the bound $r_\mathrm{HOR} \lesssim 0.1$. Thus if the other ~ 40 e-folds of inflation can be generated by some other mechanism, then single-field inflation with small field excursions can generate an observable tensor signal without violating the Lyth bound [15]. On the other hand, the smallness of the observational window also allows us to exploit another loophole in the derivation of the Lyth bound, namely the assumption that ϵ increases monotonically. This seems a natural assumption given that during inflation $\epsilon \ll 1$ and at the end of inflation $\epsilon \sim 1$; current observational constraints also strongly favour ϵ increasing during the ~ 8 e-folds of the CMB observational window. However, outside this window the behaviour of ϵ is not constrained and the assumption of monotonicity is not strictly necessary. Relaxing this assumption makes it possible to construct a scalar potential for a single field that violates the Lyth bound.

This loophole was first exploited in [16], where a fifth-order polynomial form for the scalar potential was used to generate observably large r (as large as $r = 0.1$) with ~ 60 e-folds of inflation, while matching the WMAP constraints on the amplitude, spectral tilt and running of the scalar power spectrum [21] *at the pivot scale*, all with field excursion $\Delta\phi \lesssim M_\mathrm{P}$. Supersymmetric models using a similar principle but with an additional hybrid mechanism to bring inflation to an end have also been studied [17–20], where the relevant contributions to the potential arise from quadratic and quartic terms in the inflaton field ϕ with opposite coefficients. These were matched to observational constraints from WMAP in a similar manner, and values of $r \sim 0.03$ were obtained.

However, the behaviour of $\epsilon(\phi)$ that is necessary in order to evade the Lyth bound and satisfy observational constraints in a complete inflationary model can be quite complicated, as we discuss below. In general it is not sufficient to simply match the parameters of the scalar power spectrum at the WMAP pivot scale, as done in [16–20].

2.1 The necessary features in ϵ

To violate the bound in eq. (2.7) ϵ must decrease at some point during the inflationary epoch.[2] Unfortunately this alone is not enough to successfully evade the Lyth bound and match all observations. To achieve both, a complete small-field model must have the following features:

1. At CMB scales ϵ must be large enough to generate an observable value of r.

2. ϵ must *increase* over the ~ 8 e-fold observational window.

3. After observable scales have left the horizon, ϵ must quickly decrease.

4. ϵ must eventually increase again to end inflation.

Condition (2) is dictated by a combination of the spectral index constraint from WMAP [21] and the observed value of σ_8 from large-scale structure (e.g. galaxy clusters, see [22]), which means the spectrum must decrease over the observational window.[3] The quick decrease of ϵ required in condition (3) is necessary to generate enough e-folds of inflation. If instead ϵ decreases gradually, it will need to eventually decrease to a much smaller value because $\epsilon \propto \Delta\phi/\Delta N$ and we require $\Delta\phi \leq M_P$. The change in ϵ must also not be too sharp in order to not violate slow-roll. Note that a *complete* model of inflation also requires a stable vacuum state in which $V' \to 0$.

Achieving all of these conditions with a single potential is difficult, and a viable model would require a fifth-order polynomial form for the potential, as in [16]. The most demanding aspect of the conditions is that the single scalar potential *both* dramatically reduces ϵ after observable scales leave the horizon and subsequently dramatically increases ϵ to end inflation. If inflation is instead brought to an end by another mechanism, such as a hybrid transition, as in [17–20], condition (4) is not required. This makes the task of constructing the potential simpler.

In fact, the condition that ϵ first increases and then decreases is not uncommon and can be achieved by simply adding a constant vacuum energy term to a potential that already supports inflation (and has increasing ϵ). Before the constant term becomes completely dominant ϵ will continue to increase as before. Then, when the constant term does come to completely dominate, $\epsilon \to 0$. For a large enough vacuum term, this transition will occur before $\epsilon > 1$. Of course to successfully evade the Lyth bound as described above, the occurrence of this feature must coincide with the end of the observational window and occur with the right magnitude, which is not guaranteed. However, the non-monotonic behaviour of ϵ will be. Refs. [17–20] are examples of this mechanism in action, as is our model in section 3.2.

2.2 Typical observational features

Unlike most models of inflation, models with non-monotonic evolution of ϵ will not reproduce an exact power-law spectrum of primordial density perturbations. Apart from an observable tensor-to-scalar ratio, which is obtained by design, such models generically exhibit the following two features:

1. A non-negligible, scale-dependent running, of the scalar spectral index.

2. A significant increase in the primordial power spectrum on very small scales.

---

[2]This is clear from eq. (2.6) where, if ϵ decreases, ΔN will increase for the same field excursion, $\Delta\phi$.

[3]When running of the spectral index is allowed, the best fit value for the spectral index is indeed $n_s > 1$, but the running is $\alpha < 0$, therefore ϵ must still increase eventually. Also, the value of σ_8 measured independently from LSS strongly favours a primordial spectrum that decreases in amplitude between WMAP and LSS scales.

The non-negligible running arises because there must be significant evolution of ϵ while observable scales are crossing the horizon. While it is possible in principle for all the evolution of ϵ to occur only after the observable scales have crossed the horizon, this requires *very* sharp features in ϵ since, as mentioned above, the later the decrease in ϵ begins, the greater the over-all decrease must be in order to maintain inflation for sufficient e-folds. If ϵ decreases too much, the perturbative treatment of the scalar fluctuations, and hence the consistency of inflation, breaks down.[4] Even if the parameters of the model are chosen in order to impose a small running *at the WMAP pivot scale* (as in [16–20]) the necessary evolution of ϵ required for consistency means that the running cannot remain small over the observational window, i.e., the running will be *scale-dependent*.

This means the description of the scalar power spectrum using the simple power-law model is not appropriate for models implementing such an evolution of ϵ to evade the Lyth bound. As a result, the value of σ_8 actually measured from LSS observations would be different to that inferred from the CMB if the data were analysed assuming a power-law spectrum.

Finally, the increase in the spectrum at very small scales is a result of the necessary decrease of ϵ outside the observational window. If the amplitude of the spectrum on these scales is large enough, primordial black holes (PBHs) will be formed. Current cosmological constraints on PBH's restrict $\mathcal{P}_\zeta \lesssim 10^{-2}$ (see e.g. [24–26]).

Currently, none of these features have definitely been observed, which serves to place constraints on what small-field models can circumvent the Lyth bound. On the other hand, if primordial gravitational waves were to be observed, subsequent detection of any of these features would allow us to distinguish between small-field models and other inflationary models which can generate large tensor signals.

3 A well-motivated potential

In the previous section we have discussed in very general terms the conditions that must be satisfied by any small-field model of inflation that circumvents the Lyth bound to produce a large tensor signal. We now illustrate these properties with a concrete example of a well-motivated scalar potential that can be obtained from a fundamental physics framework.

A model of inflation based on gauge invariant MSSM (minimal supersymmetric Standard Model) flat-direction fields was introduced in [27], where inflation occurs about a point of inflection in the potential. In all of these models the inflaton carries the Standard Model charges and inflation ends in a vacuum where the MSSM gauge group is restored. Therefore the inflaton decay naturally excites all the MSSM degrees of freedom [28].

This model was subsequently extended to include a constant vacuum energy term arising from the next-to-minimal supersymmetric Standard Model (NMSSM) [29, 30],[5] such that the potential was stable under radiative corrections and did not require excessive fine-tuning to reproduce a power spectrum consistent with observations.

The potential in this model can be easily parameterized by

$$V(\phi) = V_0 + A\phi^p - B\phi^q + C\phi^s , \qquad (3.1)$$

while the hybrid field remains trapped in the false vacuum. Although in principle the three powers in the potential can take many values, for the purpose of illustration here we will use $p = 2$, $q = 6$ and $s = 10$. We will assume here that the hybrid transition brings inflation to an end after the appropriate number of e-folds, so that no constraint is required on the value of ϵ at the end of inflation. The details of the embedding of this potential into a model of particle physics imposes constraints upon the the values of V_0, A, B and C. In this section we first deal with the model as a general framework, and then point out one potential embedding of the model in section 3.2.

---

[4]This can only be overcome by a concurrent sharp drop in the energy scale of inflation. Such a sharp change would be more suitably described as an inflationary model with multiple periods of inflation [23], rather than one period with an evolving ϵ.

[5]The constant term in this potential could also arise from the vacuum energy density present within a gravity mediated supersymmetry breaking sector [31], or within the MSSM-landscape [32]. These require a mechanism other than a hybrid transition to end inflation and remove the vacuum term.

To start with, the observables we choose our model to reproduce are: the amplitude of the scalar power spectrum, A_k, the scalar spectral index, n_s and the tensor to scalar ratio, r, at the WMAP pivot scale $k_{\text{piv}} = 0.002 \text{ Mpc}^{-1}$. In section 3.1 we examine the spectrum produced by this model beyond this power-law assumption. For a given potential $V(\phi)$, when the field is slowly rolling and takes field value ϕ_{CMB} these observables are given by

$$A_k = \frac{V(\phi_{\text{CMB}})}{24\pi^2 \epsilon(\phi_{\text{CMB}})}, \tag{3.2}$$

$$n_s = 1 + 2\eta(\phi_{\text{CMB}}) - 6\epsilon(\phi_{\text{CMB}}) \tag{3.3}$$

and

$$r = 16\epsilon(\phi_{\text{CMB}}). \tag{3.4}$$

We choose ϕ_{CMB} to be the field value at which the pivot scale k_{piv} crosses the horizon. Conveniently, these equations can be re-arranged to give $V(\phi_{\text{CMB}})$, $V'(\phi_{\text{CMB}})$ and $V''(\phi_{\text{CMB}})$ as a function of the observable quantities

$$V(\phi_{\text{CMB}}) = \frac{3}{2}(A_k r \pi^2), \tag{3.5}$$

$$V'(\phi_{\text{CMB}}) = \frac{3}{2}(A_k r \pi^2)\sqrt{\frac{r}{8}} \tag{3.6}$$

and

$$V''(\phi_{\text{CMB}}) = \frac{3}{4}\left(\frac{3r}{8} + n_s - 1\right)(A_k r \pi^2). \tag{3.7}$$

Therefore, for any chosen ϕ_{CMB} and V_0, we obtain a matrix equation for the variables A, B and C:

$$\begin{pmatrix} \phi_{\text{CMB}}^2 & -\phi_{\text{CMB}}^3 & \phi_{\text{CMB}}^4 \\ 2\phi_{\text{CMB}} & -3\phi_{\text{CMB}}^2 & 4\phi_{\text{CMB}}^3 \\ 2 & -6\phi_{\text{CMB}} & 12\phi_{\text{CMB}}^2 \end{pmatrix} \begin{pmatrix} A \\ B \\ C \end{pmatrix} = \begin{pmatrix} V(\phi_{\text{CMB}}) - V_0 \\ V'(\phi_{\text{CMB}}) \\ V''(\phi_{\text{CMB}}) \end{pmatrix}. \tag{3.8}$$

This is easily inverted to find the required values of A, B and C, and thus the complete potential, $V(\phi)$. Note that the slow-roll constraints $\epsilon \ll 1$ and $|\eta| \ll 1$ are automatically satisfied at ϕ_{CMB}, but there is no guarantee that the generated potential will be able to generate the minimum required number of e-folds of inflation, N_{req}. This must be checked for each chosen value of ϕ_{CMB} and V_0. There is also no guarantee that for all N_{req} e-folds A_k, n_s and r will remain close to their values at ϕ_{CMB}.

Using this method, we have reduced the numerical difficulty to a two-dimensional problem. Having chosen the observational parameters we wish to match, we need only scan over the two parameters V_0 and ϕ_{CMB} to find a potential that can sustain inflation for $> N_{\text{req}}$ e-folds. The waterfall transition that ends inflation is then restricted to occur exactly N_{req} e-folds after $\phi = \phi_{\text{CMB}}$. As a test of the method we will show that it is possible to obtain:

$$r = 0.05, \quad n_s = 0.98, \quad A_k(k_{\text{piv}}) = 2.3 \times 10^{-9}, \quad \text{for } N_{\text{req}} = 50, \quad \text{and} \quad \phi_{\text{CMB}} = M_{\text{P}}. \tag{3.9}$$

The values of n_s and A_k are the WMAP 7-year best fit values for a power-law scalar spectrum with non-zero tensor spectrum [21]. As noted above, the power spectrum thus produced will generically differ significantly from a power-law form. Therefore we further require that the power at very small scales is always $\mathcal{P}(k) \leq 10^{-2}$ during inflation, to ensure there is no over production of PBH's [24]. The final constraint imposed is that the power at $k = 0.3 \text{ Mpc}^{-1}$ is not more than 10% different than that for a power-law spectrum with $n_s = 0.98$. Note that $k = 0.3 \text{ Mpc}^{-1}$ corresponds to multipole $l > 3000$. Although the precise scale at which this matching is imposed is somewhat arbitrary, this constraint is necessary to ensure that the model does not predict too much power on intermediate scales, which would conflict with LSS observations of σ_8 [22] and measurements of the small scale angular power spectrum of the CMB from, e.g., QUaD [33], ACBAR [34] and Boomerang [35].
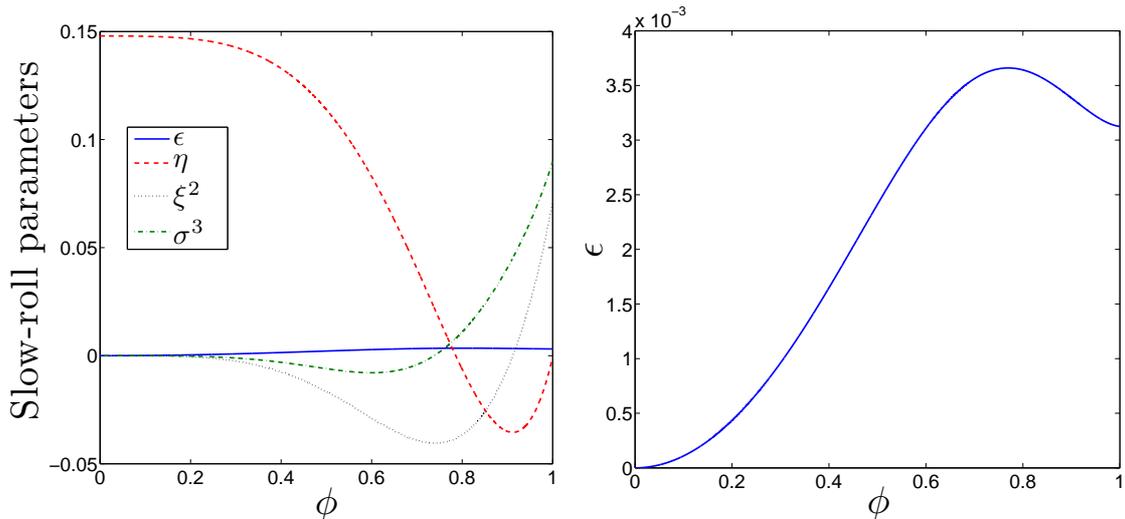
Figure 1. *Left panel*: The behaviour of the slow-roll parameters as a function of inflaton field value ϕ, measured in units of M_{P}, for the model parameters given in equation (3.10). *Right panel*: ϵ as a function of ϕ for the same parameters, shown with a magnified scale.

A particular choice of V_0 which satisfies all of these constraints produces the following parameters:

$$V_0^{1/4} = 0.0063 M_{\mathrm{P}}, \quad A = 1.19 \times 10^{-10} M_{\mathrm{P}}^2, \quad B = 2.87 \times 10^{-11} M_{\mathrm{P}}^{-2}, \quad C = 6.90 \times 10^{-12} M_{\mathrm{P}}^{-6}. \quad (3.10)$$

For these parameters, figure 1 shows the behaviour of the slow-roll parameters ϵ, η, ξ^2 and $\sigma^3 \equiv M_{\mathrm{P}}^6 V'^2 (d^4 V / d\phi^4)/V^3$ as a function of ϕ. It is clear that the required evolution of $\epsilon(\phi)$, outlined in section 2.1, is satisfied. Note that the ordinary slow-roll hierarchy is not maintained due to the non-monotonic behaviour of ϵ, and that the other slow-roll parameters themselves show non-monotonic behaviour. The power spectrum will therefore differ from the standard power-law form, and in general the slow-roll approximation for calculating the power spectrum will not be valid.

3.1 Predictions beyond slow-roll and a power-law spectrum

The predicted power spectrum obtained from the slow-roll approximation will be correct to the same order as the slow-roll parameters themselves. Therefore, if the higher order slow-roll parameters ξ^2, σ^3 etc. are generically large, the corrections to the predicted power spectrum might also be large. In order to check this we calculate the spectrum numerically. To do this we assume the Bunch-Davies vacuum state and numerically integrate the scale factor, field value and curvature perturbation from deep inside the horizon until well after horizon exit using the equation of motion given by linear perturbation theory [36]. Figure 2 shows $\mathcal{P}(k)$ calculated by the two different methods. At small scales the deviation is significant. Even at large scales, as shown in the inset to figure 2, these differences are of order 5% or more, and for different choice of model parameters may be more significant than this. For all subsequent plots we therefore use the full numerical calculation of $\mathcal{P}(k)$ rather than the slow-roll approximation.

It is also instructive to compare the power spectrum obtained from the full numerical calculation for this model with the power-law spectrum with $A_k = 2.3 \times 10^{-9}$ and $n_s = 0.98$. These were the parameters of the power spectrum to which we had matched our model at the WMAP pivot scale. Despite this matching at k_{piv} and the additional matching (to within 10%) at $k = 0.3$ Mpc^{-1}, the fractional difference in the power spectrum compared to the assumed power-law form can become significant over the range of scales constrained by current CMB measurements, as shown in figure 3. This shows that a power-law is not the ideal framework with which to analyse the power spectrum generated in this model.
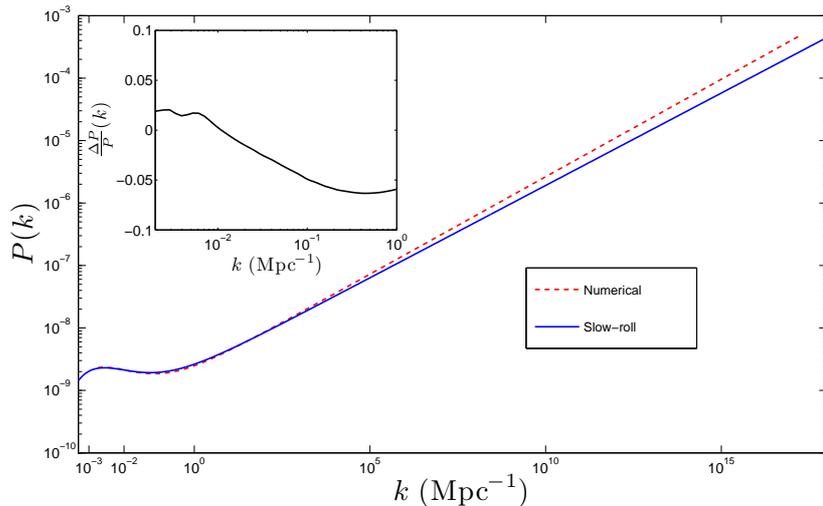
Figure 2. Power $P(k)$ for the model parameters of equation (3.10) for the entire range of scales k that cross the horizon during the $N_{\rm req}$ e-folds of inflation. The solid blue curve is obtained from the slow-roll approximation and the red dashed curve from a full numerical calculation. *Inset*: The fractional difference $(P_{\rm num} - P_{\rm s.r.})/P_{\rm num}$ between the numerical calculation and the slow-roll approximation at large scales corresponding to the current observational window.
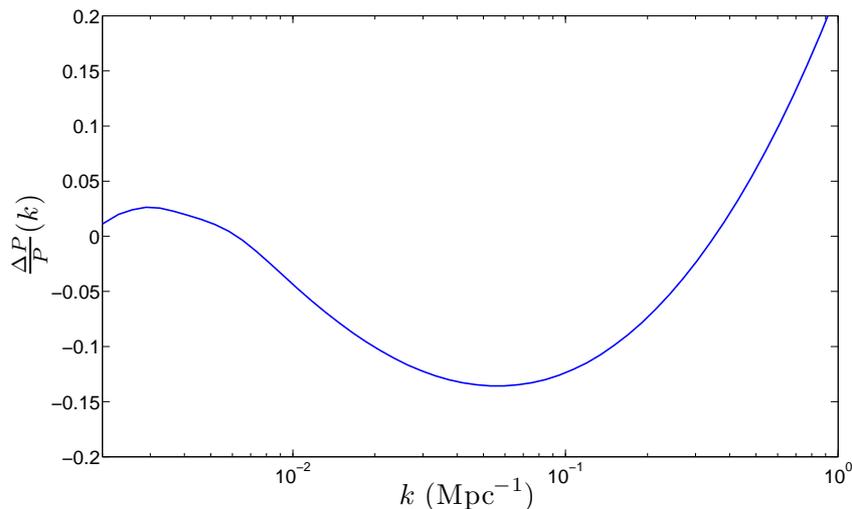

Figure 3. The fractional difference between the numerically evaluated power spectrum $P(k)$ for parameters in equation (3.10) and the assumed power-law form with the values of $A_k = 2.3 \times 10^{-9}$ and $n_s = 0.98$ at the pivot scale $k_{\rm piv} = 0.002$ Mpc^{-1} to which the model was matched as described in the text.

For the parameters we have chosen in eq. (3.10), the two spectra match to within 20% over the WMAP constrained range. This is equivalent to the accuracy quoted in the parameter A_k when both tensors and running are included in the WMAP analysis [21]. Therefore such a form of the primordial power will be within current constraints, but should be possible to distinguish when using the tighter constraints expected from Planck.

This deviation from a power-law form of the power spectrum is an important feature of our model and in fact is a generic feature of *any* small-field model generating observable gravitational waves. This has not been accounted for in previous analyses of small-field models of inflation generating large
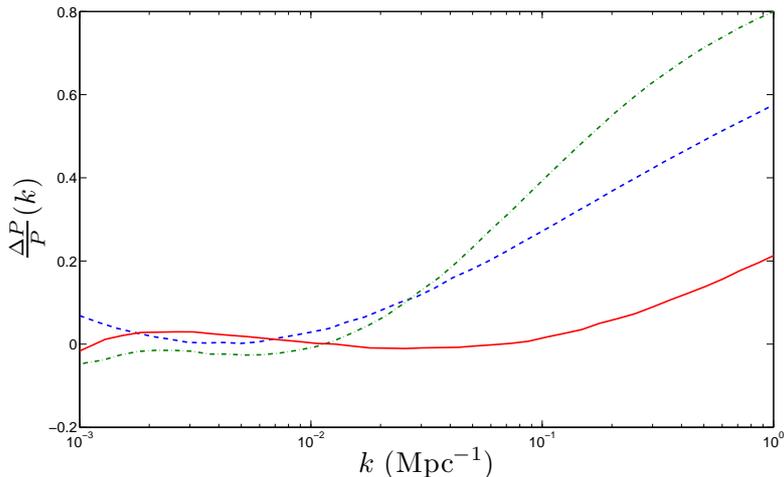
Figure 4. The fractional difference between the numerically evaluated power spectrum $P(k)$ and the assumed power-law form to which the values of A_k, n_s and α are matched at the pivot scale $k_{\rm piv} = 0.002$ Mpc^{-1}. The green dash-dot curve is for model 1, the blue dashed curve for model 2 and the red solid curve for model 3. The various models are described in section 3.1. Model 1 is taken from [16] and model 2 from [18]. Note that although the power spectra are matched to the power-law form at the pivot scale, they all necessarily deviate from this form at other scales within the observational window. Only model 3 matches the power-law to within current observational accuracy.

r. To demonstrate this, we consider two different models from the literature. The first model is based on the fifth-order polynomial form for $V(\phi)$ considered in [16], which gives a tensor-to-scalar ratio $r = 0.02$. The parameter values are taken from Table 1 in [16] (second line) and have been chosen in order to match the power spectrum to that of a power law with $A_k = 2.3 \times 10^{-9}$, $n_s = 0.99$ and $\alpha = 0.001$ at the pivot scale $k_{\rm piv}$. We refer to this as model 1. The second model, referred to as model 2, is based on the model of supersymmetric hybrid inflation considered in [18]. The relevant portion of the potential for this model is

$$V(\phi) = V_0 \left(1 + \frac{|\kappa_s|}{M_{\rm P}^2} \phi^2 + \frac{\gamma_s}{2 M_{\rm P}^4} \phi^4 \right) \tag{3.11}$$

at the time of generation of the CMB perturbations (for more details, see [18]). We choose the parameter values for this potential in order to obtain $r = 0.02$, $A_k = 2.3 \times 10^{-9}$, $n_s = 0.96$ and $\alpha = 0.003$ at $k_{\rm piv}$ (which is assumed to cross the horizon at $\phi_{\rm CMB} = 0.5 M_{\rm P}$). This results in $V_0 = 6.7 \times 10^{-10} M_{\rm P}^4$, $|\kappa_s| = 0.08$, $\gamma_s = -0.118$. Note that the parameters of these models are chosen as examples which both generate the same value of r. In figure 4, we plot as a function of the scale k the fractional difference between the numerically evaluated power spectrum $\mathcal{P}(k)$ for each of these models and the power-law form of the power spectrum (with scale-independent running) to which they are matched at the pivot scale. For comparison, we include the same plot for parameter values

$$V_0^{1/4} = 0.0051 M_{\rm P}, \quad A = 3.54 \times 10^{-11} M_{\rm P}^2, \quad B = 1.75 \times 10^{-11} M_{\rm P}^{-2}, \quad C = 8.81 \times 10^{-12} M_{\rm P}^{-6}. \tag{3.12}$$

for our model of equation (3.1) (here $\phi_{\rm CMB} = 0.8\, M_{\rm P}$). These parameter values are chosen to obtain $r = 0.02$, $A_k = 2.3 \times 10^{-9}$, $n_s = 0.96$ and $\alpha = 0.001$ at $k_{\rm piv}$ and thus correspond closely to model 2. We refer to this as model 3.

From figure 4 it is obvious that all three models result in scalar power spectra that deviate from the power-law form at intermediate or small scales even when they are explicitly matched to a power-law spectrum at large scales. As explained in section 2.2, this is to be expected as a generic feature of any small-field model generating observable gravitational waves. It is therefore not appropriate to

merely match the power spectrum to a power-law at k_{piv}: both models 1 and 2, which have been claimed to match observational constraints on the scalar power spectrum, in fact predict a significant excess of power at scales of $k \simeq 0.1$ Mpc^{-1}, which will put them in tension with σ_8 measurements. Note that model 3, although certainly not a power-law, is the only model of the three that matches the power-law to within current observational accuracy.

If a large r is observed along with a large running, then it will be possible to directly compare the goodness of fit of our model's spectrum and a simple running power-law. For the running power-law there are four free parameters. These are r, A_k, n_s and $\alpha = \mathrm{d}n_s/\mathrm{d}\ln k$. For the model presented in this paper there also four parameters. These are V_0, A, B and C. In principle, because our model requires other physics to end inflation there is one additional parameter. This is either ϕ_{CMB} or ϕ_{e}. However, the extra constraints we impose that $\phi_{\text{CMB}} \lesssim M_{\text{P}}$ and that the spectrum at the smallest scales is less than 10^{-2}, strongly constrains this extra parameter. Also, if the effects of PBH's were to be observed, this would provide a fifth observable for our model.

It is also interesting to note that if PBH's are generated at the correct scales, then they can be a viable dark matter candidate [24, 26]. In ordinary inflation models it is difficult to generate enough power to create PBH's, whereas in our model it is difficult not to. Nevertheless, a full exploration of the implications of this although interesting is well beyond the scope of the present work.

3.2 The model embedded within supergravity using MSSM flat directions

In this section we describe a simple particle theory embedding for the scalar potential of the form of equation (3.1). This potential can be obtained within the MSSM where there are D-flat directions which are lifted by non-renormalizable operators (for a review see [37]). At high scales, the supergravity corrections dominate the soft-supersymmetry breaking contribution of the inflaton potential, as suggested in [31]. The MSSM potential obtains leading corrections which are dominated by the Hubble-induced terms. The total potential is given by (see [31, 38]):

$$V = V_0 + c_H H^2 |\phi|^2 - a_H \lambda_n H \frac{\phi^6}{M_{\text{P}}^3} + \lambda_n^2 \frac{|\phi|^{10}}{M_{\text{P}}^6} \tag{3.13}$$

where $V_0 = 3H^2 M_{\text{P}}^2$, c_H and a_H are numerical factors arising from supergravity corrections. We will work with the assumption that c_H, $a_H \sim \mathcal{O}(1 - 100)$. Note that the Hubble-induced corrections match the expressions given in eqs.(3.1) and (3.10) with appropriate values of V_0, A, B, C. We can ignore the soft terms such as m_ϕ as compared to the Hubble-induced terms.[6] By comparing to our sample point, we can read off the parameters that correspond to (3.10). These are:

$$H = 3.5 \times 10^{11} \text{ GeV}, \quad c_H \sim 8.2, \quad a_H \sim 76, \quad \lambda_n \sim 2.6 \times 10^{-6}. \tag{3.14}$$

Our analysis suggests that in order to realize a large tensor-to-scalar ratio, $r \sim 0.05$, we would require a small value for of λ_n. This is the coefficient of the non-renormalizable operator for the MSSM flat directions, such as **udd** and **LLe** [27] (**u** and **d** are the right handed squarks, **L** is the left handed slepton while **e** corresponds to the right handed selectron). The other coefficients, c_H and a_H are within the allowed range of supergravity corrections arising from the mixing of the Kähler potential and superpotential. However, the non-renormalizable interaction, λ_n turns out to be unnaturally small. Both **udd** and **LLe** carry global $U(1)$ numbers, and in both the cases it is expected that $U(1)$ would be broken by quantum gravity effects with order unity, i.e. $\lambda_n \sim \mathcal{O}(1)$. However, it is not unforeseeable that due to some reasons quantum gravity effects break the global baryon or lepton number operators *softly*. Inspite of this challenge it is still nice to see that it is possible to obtain a large tensor-to-scalar ratio in a model where $\Delta\phi \leq M_{\text{P}}$ and the end of inflation creates *solely* the MSSM degrees of freedom, therefore creating a thermal bath with all the Standard Model quarks and leptons, and also the dark matter component as the lightest supersymmetric particle [39].

---

[6]Note that the effective mass term is now governed by the large Hubble-induced mass term. Therefore in this model there is no supergravity-η problem.

4 Summary and Discussion

In this paper we have discussed small-field models of inflation that can generate observably large gravitational waves. As has been noted in [15–20], if a significant tensor-to-scalar ratio is observed through the CMB this does not rule out small-field inflation. This result does not contradict the well known Lyth bound because it does not satisfy one of the assumptions used to derive this bound, namely that ϵ increases monotonically during inflation.

We have discussed the generic features that $\epsilon(\phi)$ must possess in such models in order to meet observational constraints, and the distinct observational signatures any non-monotonic ϵ model will produce. The most important of these are a scale-dependent running of the scalar spectral index and an enhancement of power on very small scales, potentially leading to the formation of primordial black holes. As a result of the scale-dependent running of the spectral index, the primordial power spectrum generally differs from the power-law form usually assumed so it is not appropriate to fit the spectrum to the data at one scale assuming such a form. Some previous examples discussed in the literature [16–20] have not taken this into account and so may be more constrained by CMB observations than was previously realised.

A deviation of the primordial power spectrum from a power-law form may be inferred from the data if σ_8 measurements from large-scale structure were to be found to disagree with those predicted from CMB data when analysed assuming a power-law spectrum. If indeed a tensor signal were to be observed in the future, such a scale-dependent running and primordial black holes would be a smoking gun signal with which to distinguish these small-field inflation models from other models which can also generate large r.

We have argued that the required behaviour in ϵ is relatively common when a constant vacuum energy is added to a potential that supports inflation and a hybrid mechanism is included to bring inflation to an end. We have also discussed a small-field model which implements this mechanism. We have shown the existence of a point in the parameter space of this model with $r = 0.05$ that predicts a scalar power spectrum $\mathcal{P}(k)$ which deviates from the current best-fit power-law by less than 20% over all the currently observed range of k values. When a tensor signal and running of the scalar spectral index is included, this is the accuracy to which the WMAP data can constrain the amplitude of the running power-law spectrum. We conclude that our model will not be able to give a fit to current data that is statistically better or worse with any significance compared to a running power-law model, because there is not enough information in the data. However, if a future CMB observation, perhaps from Planck, were to measure both r and α with statistical significance, a full Markov Chain Monte Carlo (MCMC) analysis of our model could provide useful information.

Additionally, we observed that the generation of primordial black holes after inflation is a generic feature of non-monotonic ϵ models. The fact that these have not yet been observed provides tight constraints on the allowed parameter space and effectively fully constrains one free parameter of the model. We have not explored this observational feature beyond using it as a constraint; however it would appear to be an interesting avenue for future pursuits.

Although the scalar potential we have discussed satisfies current observational constraints, embedding it in a fundamental physics model is not without difficulty. We have provided an example of how this may occur within an MSSM framework, but in this implementation the coefficient of one term in the potential must take small values. The initial conditions of this model also need to be delicately arranged if slow-roll inflation is to occur, possibly through the dynamical mechanism suggested in [40]. This is also true of other small-field models in the literature. Nevertheless, the fine-tuning problems of these small-field models appear to be no greater than those arising in reconciling large-field models with fundamental theory. Therefore, although from a theoretical perspective large r values may be disfavoured, if a primordial tensor signal were in fact to be observed then contrary to popular wisdom small-field models should be considered at least as seriously as large-field models. Thankfully, due to their distinct observational signatures, the choice between them then need not be based on theoretical prejudice alone.

Acknowledgments

References

[1] L. P. Grishchuk, Sov. Phys. JETP **40**, 409-415 (1975). A. A. Starobinsky, Sov. Astron. Lett. **11**, 133 (1985). B. Allen, Phys. Rev. **D37**, 2078 (1988). V. Sahni, Phys. Rev. **D42**, 453-463 (1990).

[2] www.esa.int/Planck

[3] A. Mazumdar and J. Rocher, Phys. Rept. **497**, 85 (2011) [arXiv:1001.0993 [hep-ph]].

[4] D. H. Lyth, Phys. Rev. Lett. **78** (1997) 1861-1863. [hep-ph/9606387].

[5] A. D. Linde, Phys. Lett. **B129**, 177-181 (1983). A. D. Linde, Phys. Lett. **B175**, 395-400 (1986).

[6] R. Allahverdi, R. Brandenberger, F. Y. Cyr-Racine and A. Mazumdar, Ann. Rev. Nucl. Part. Sci. **60**, 27 (2010) [arXiv:1001.2600 [hep-th]].

[7] E. Silverstein, A. Westphal, Phys. Rev. **D78** (2008) 106003. [arXiv:0803.3085 [hep-th]]. L. McAllister, E. Silverstein, A. Westphal, Phys. Rev. **D82** (2010) 046003. [arXiv:0808.0706 [hep-th]].

[8] C. P. Burgess, L. McAllister, Class. Quant. Grav. **28** (2011) 204002. [arXiv:1108.2660 [hep-th]].

[9] M. Cicoli and A. Mazumdar, JCAP **1009**, 025 (2010) [arXiv:1005.5076 [hep-th]]. M. Cicoli and A. Mazumdar, Phys. Rev. D **83**, 063527 (2011) [arXiv:1010.0941 [hep-th]].

[10] A. R. Liddle, A. Mazumdar and F. E. Schunck, Phys. Rev. D **58**, 061301 (1998) [arXiv:astro-ph/9804177]. E. J. Copeland, A. Mazumdar and N. J. Nunes, Phys. Rev. D **60**, 083506 (1999) [arXiv:astro-ph/9904309].

[11] P. Kanti, K. A. Olive, Phys. Rev. **D60**, 043502 (1999). [hep-ph/9903524]. P. Kanti, K. A. Olive, Phys. Lett. **B464**, 192-198 (1999). [hep-ph/9906331].

[12] A. Jokinen and A. Mazumdar, Phys. Lett. B **597**, 222 (2004) [arXiv:hep-th/0406074].

[13] A. Mazumdar, S. Panda and A. Perez-Lorenzana, Nucl. Phys. B **614**, 101 (2001) [arXiv:hep-ph/0107058].

[14] S. Dimopoulos, S. Kachru, J. McGreevy, J. G. Wacker, JCAP **0808**, 003 (2008). [hep-th/0507205].

[15] S. Hotchkiss, G. German, G. G. Ross, S. Sarkar JCAP **0810**, 015 (2008). [arXiv:0804.2634 [astro-ph]].

[16] I. Ben-Dayan, R. Brustein, JCAP **1009**, 007 (2010). [arXiv:0907.2384 [astro-ph.CO]].

[17] Q. Shafi, J. R. Wickman, Phys. Lett. **B696** (2011) 438-446. [arXiv:1009.5340 [hep-ph]].

[18] M. U. Rehman, Q. Shafi, J. R. Wickman, Phys. Rev. **D83** (2011) 067304. [arXiv:1012.0309 [astro-ph.CO]].

[19] N. Okada, M. U. Rehman, Q. Shafi, Phys. Lett. **B701** (2011) 520-525. [arXiv:1102.4747 [hep-ph]].

[20] M. Civiletti, M. U. Rehman, Q. Shafi, J. R. Wickman, [arXiv:1104.4143 [astro-ph.CO]].

[21] E. Komatsu *et al.* [WMAP Collaboration], Astrophys. J. Suppl. **192**, 18 (2011).

[22] A. Mantz, S. W. Allen, D. Rapetti and H. Ebeling, Mon. Not. Roy. Astron. Soc. **406** (2010) 1759 [arXiv:0909.3098 [astro-ph.CO]].

[23] J. A. Adams, G. G. Ross and S. Sarkar, Nucl. Phys. B **503** (1997) 405 [arXiv:hep-ph/9704286].

[24] B. J. Carr, K. Kohri, Y. Sendouda and J. Yokoyama, Phys. Rev. D **81**, 104019 (2010) [arXiv:0912.5297 [astro-ph.CO]].

[25] L. Alabidi and K. Kohri, Phys. Rev. D **80**, 063511 (2009) [arXiv:0906.1398 [astro-ph.CO]].

[26] M. Drees, E. Erfani, JCAP **1104** (2011) 005. [arXiv:1102.2340 [hep-ph]]

[27] R. Allahverdi, K. Enqvist, J. Garcia-Bellido and A. Mazumdar, Phys. Rev. Lett. **97**, 191304 (2006) [arXiv:hep-ph/0605035]. R. Allahverdi, A. Kusenko and A. Mazumdar, JCAP **0707**, 018 (2007)

[arXiv:hep-ph/0608138]. R. Allahverdi, K. Enqvist, J. Garcia-Bellido, A. Jokinen and A. Mazumdar, JCAP **0706**, 019 (2007) [arXiv:hep-ph/0610134]. A. Chatterjee, A. Mazumdar, JCAP **1109**, 009 (2011). [arXiv:1103.5758 [hep-ph]].

[28] R. Allahverdi, A. Ferrantelli, J. Garcia-Bellido and A. Mazumdar, Phys. Rev. D **83** (2011) 123507 [arXiv:1103.2123 [hep-ph]].

[29] S. Hotchkiss, A. Mazumdar and S. Nadathur, JCAP **1106**, 002 (2011) [arXiv:1101.6046 [astro-ph.CO]].

[30] K. Enqvist, A. Mazumdar and P. Stephens, JCAP **1006**, 020 (2010) [arXiv:1004.3724 [hep-ph]].

[31] A. Mazumdar, S. Nadathur and P. Stephens, arXiv:1105.0430 [hep-th].

[32] A. Mazumdar and S. Nadathur, arXiv:1107.4078 [hep-ph].

[33] S. Gupta *et al.* [QUaD collaboration], Astrophys. J. **716** (2010) 1040 [arXiv:0909.1621 [astro-ph.CO]].

[34] C. L. Reichardt, P. A. R. Ade, J. J. Bock, J. R. Bond, J. A. Brevik, C. R. Contaldi, M. D. Daub, J. T. Dempsey *et al.*, Astrophys. J. **694** (2009) 1200-1219. [arXiv:0801.1491 [astro-ph]].

[35] C. J. MacTavish *et al.*, Astrophys. J. **647** (2006) 799 [arXiv:astro-ph/0507503].

[36] V. F. Mukhanov, H. A. Feldman, R. H. Brandenberger, Phys. Rept. **215** (1992) 203-333.

[37] K. Enqvist, A. Mazumdar, Phys. Rept. **380**, 99-234 (2003). [arXiv:hep-ph/0209244 [hep-ph]].

[38] S. Kasuya, M. Kawasaki, Phys. Rev. **D74**, 063507 (2006). [hep-ph/0606123].

[39] R. Allahverdi, B. Dutta and A. Mazumdar, Phys. Rev. D **75**, 075018 (2007) [arXiv:hep-ph/0702112].

[40] R. Allahverdi, B. Dutta and A. Mazumdar, Phys. Rev. D **78** (2008) 063507 [arXiv:0806.4557 [hep-ph]]. K. Kamada, J. Yokoyama, Prog. Theor. Phys. **122** (2010) 969-986. [arXiv:0906.3402 [hep-ph]].